Ionics (2019) 25:3761–3768
https://doi.org/10.1007/s11581-019-02938-1

ORIGINAL PAPER

Synthesis of polyaniline and application of hydrophobic breathable structure in zinc–polyaniline battery

Dan-Dan Sun[1] · Jia-Jun Han[1] · Hui Ma[2] · Ning Zhang[1] · Tao Han[1] · Jin-Ning Cheng[1]

Received: 9 December 2018 / Revised: 17 February 2019 / Accepted: 18 February 2019 / Published online: 22 March 2019

Abstract

A polyaniline/carbon (PANI/C) composite material was synthesized by chemical oxidation polymerization method and was manufactured to the form of gas diffusion electrode inspired by a zinc–air battery, and was used as cathode material. The composite's structure and morphology of the synthesized polyaniline (PANI) composites were characterized by Fourier-transform infrared spectroscopy, X-ray diffraction, and field-emission scanning electron microscopy. The electrochemical properties of the electrodes were examined by electrochemical impedance spectroscopy (EIS), polarization curves, and galvanostatic discharge. The cell voltage kept at 0.88 V for 100 h during the galvanostatic discharge progress at the current of 10 mA and the specific discharge capacity achieved 1850 mAh/g which was 10 times more than the theory value of traditional Zn–PANI battery (about 100–200 mAh/g at the current density of 0.5 mA/cm^2). Polyaniline acts as a special catalyst to catalyze oxygen reduction to achieve large capacity.

Keywords Polyaniline · Hydrophobic permeability · Catalysis · Discharge · High specific capacity

Introduction

Since the end of the last century, unprecedented energy consumption and global climate change are two major problems facing the world. At present, fossil fuels are still the most mainstream energy source which will eventually become exhausted with the significant increase in energy demand. As mentioned above, the development and use of renewable energy are the key to solving the problem. However, the power output of new energy sources such as solar energy, wind energy, and tidal energy is greatly affected by external factors such as season, climate, and location [1–3]. It is difficult to meet people's requirements for the timeliness and ease of use of energy. Chemical power supplies are gaining more and more attention as high-efficiency energy conversion devices [4–7].

Zinc is a non-toxic, relatively inexpensive, and abundant material whose low (negative) electrode potential and high hydrogen overpotential make it a very suitable anode material for aqueous electrolytes. Zinc-based batteries are very attractive to both primary and secondary battery systems, such as Zn//MnO_2 [8, 9], Zn//air [10–12], and Zn//PANI systems [13, 14].

The conductive high molecular polymer polyaniline (PANI) has been widely used in high specific energy zinc polymer secondary batteries because of its good reversible redox capability [15–18], including polymer carbon composites and aniline copolymers [19–22]. It is composed of alternating benzene rings and anthracene rings and its conductivity can be greatly improved by doping with protic acid (hydrochloric acid, perchloric acid) which can be synthesized by chemical oxidation or electrochemical method.

In comparison with classical batteries and aprotonic cells, aqueous Zn//PANI batteries composed of PANI cathode and zinc anode with aqueous electrolyte exhibit a lot of advantages such as ecological acceptability, low cost, and easy manufacture [23, 24]. However, anions cannot enter the interior of polyaniline macromolecules, so polyaniline electrodes cannot be utilized sufficiently [25]; the capacity of zinc–polyaniline batteries is just 100–200mAh/g [5]. And studies have shown that reduced polyaniline is easily oxidized by oxygen when exposed to air. The fully reduced polyaniline hydrochloride can spontaneously undergo oxidation in the presence of air.

✉ Jia-Jun Han
hanjiajunhitweihai@163.com

[1] School of Marine Science and Technology, Harbin Institute of Technology, Weihai 264209, China

[2] Weihai Wenlong batteries Co, Ltd, Weihai, China

The color of polyaniline changes from time, first yellow brown, yellow green, and finally black green.

Pure polyaniline is prone to agglomeration, and its comprehensive performance is often not fully utilized [26, 27]. In this study, the discharge process of Zn–oxygen fuel cell was introduced into the Zn//PANI film battery because the reduced PANI film could be oxidized by oxygen and used as an O_2 "fuel-cell" type electrocatalytic electrode [28]. The gas diffusion structure of the anode in the zinc–air battery is used (as shown in Fig. 1) [29, 30]; the polyaniline and polytetrafluoroethylene (PTFE) are used together as the positive electrode, so that there are sufficient gas, liquid, and solid three-phase interfaces in the positive electrode, so that the polyaniline can be sufficiently contacted with oxygen from air. Three-dimensional (3D) meso-high density of exposed active sites, and abundant channels for porous or macroporous nanostructures possess big surface area, high density of exposed active sites, and abundant channels for mass transfer of reactants and products, thus being favorable to the oxidation of reduced PANI during the discharge process by capturing more oxygen [31–33]. In the positive electrode, polyaniline becomes a specific ORR catalyst through its own REDOX to realize long-term stable discharge. At the same time, the reduction reaction of activated carbon catalyzed oxygen will also occur to the positive electrode. We have used polyaniline synthesized by chemical oxidative polymerization to form a gas diffusion electrode to increase the capacity of the battery.

Experiment

Chemicals and materials

Aniline (AN), ammonium persulfate (APS), hydrochloric acid (37% HCl), $NH_3{\cdot}H_2O$ (28%), $MnSO_4$, $KMnO_4$, carbon paper, anhydrous sodium sulfate (Na_2SO_4), perchloric acid ($HClO_4$), activated carbon, and anhydrous alcohol are all analytical grade chemicals and purchased from the National Pharmaceutical Group Chemical Reagent Company, No. 52 Ningbo Road, Shanghai, China. Acetylene black is battery grade, purchased from Aladdin, Y891 (Branch), Fengxian District, Shanghai, China.

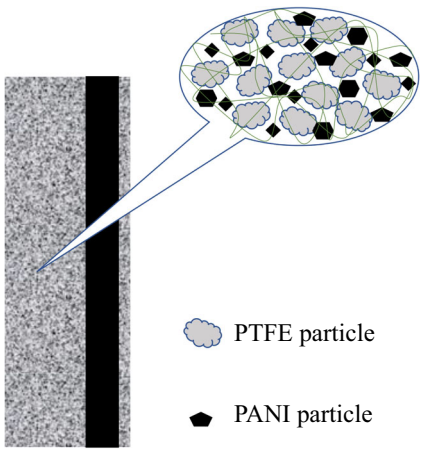

Fig. 1 The structure of hydrophobic PANI electrode

Preparation of polyaniline

Electrochemical polymerization

In order to study the oxidation of polyaniline, the polyaniline film was synthesized by electrochemical method. In 0.5 M HCl and 0.25 M aniline solution, flexible graphite paper (1 cm × 1 cm) was used as the working electrode, carbon rod was used as the counter electrode, and Hg/Hg_2SO_4 (SEE) was used as a reference electrode. Polyaniline film will be obtained by a constant current (5 mA/cm^2) for 5 min. The received polyaniline film was then washed with dilute perchloric acid and deionized water.

Chemical oxidation polymerization

In this paper, polyaniline is synthesized by adsorption double oxidant chemical oxidation method which is economical and suitable for mass production. Moreover, the synthesized polyaniline is doped with hydrochloric acid and has good electrical conductivity. The typical polymerization procedure is as follows.

First, MnO_2 precursor was prepared: dissolve 10.14 g of $MnSO_4{\cdot}H_2O$ in 50 ml of deionized water, add a drop of H_2SO_4; dissolve 6.32 g of $KMnO_4$ in 200 mL of deionized water, add a drop of $HClO_4$; drop the $MnSO_4$ solution to $KMnO_4$ solution and the addition was completed in 30 min, and the reaction was carried out in a 45 °C water bath for 2 h, then suction filtered and washed with deionized water until neutral, and then dissolved in 50 ml of deionized water for storage.

Synthesis reaction of polyaniline was proceeded in a 1000-ml reaction vessel, and 1.4 g of adsorbed carbon was added into 100 ml of water and sonicated for 30 min at least. Then, 150 g of HCl were successively added into the above mixture and stirred for 1 h. Next, 100 g of deionized ice was added into the reactor to lower temperature below 10 °C. In addition, the mixture was cooled by constant stirring in an ice bath with a temperature of 4–6 °C after the reactive monomer, 70 g of aniline was added to the reactor. Then, as-prepared initiator MnO_2 was added slowly into the well-stirred suspension for 5 to 10 min. And after 30 min, 2 g of APS per minute was added to the reactor, repeating 100 times and the temperature should stay below 5 °C simultaneously. The polymerization was undergone at 5–8 °C by adding the ice for 4 h. The resultant mixture was filtered and washed with distilled water for three times and ethanol for one time, and then further dried under

vacuum at 60 °C for 1 day to obtain the polyaniline doped with hydrochloric acid (y-PANI). Then 50 g of the obtained polyaniline wet powder (y-PANI) was added to 15 mL of aqueous ammonia, 100 mL of deionized water, and stirred at 40 °C for 24 h to obtain eigenstate polyaniline (PANI).

Preparation of positive electrode

Hydrophobic permeability is achieved in the positive electrode material by hydrophobic polytetrafluoroethylene (PTFE) and hydrophilic PANI. The PTFE (30%), activated carbon, Na_2SO_4 (20%), PANI, and acetylene black (10%) are uniformly mixed in a certain ratio, and then heated to 80° to break the emulsion and roll to a certain thickness. The sheet is attached to a current collector and pressed with a certain pressure, and then dried, and the other side is coated with PTFE as a waterproof gas permeable layer to obtain a positive electrode sheet. The polyaniline anode and battery structure are shown in Fig. 2.

Structure and morphology characterization

The XRD spectra were recorded on a D/X2700 diffractometer (Dan dong HaoYuan Instrument Co.,Ltd.,China) with Cu Kα radiation. The morphology and observation were performed on field-emission scanning electron microscopy (MERLIN Compact, Zeiss, Germany). FTIR spectra were obtained by using a Nicolet 380 FT infrared spectrometer (US Thermo Electron Corporation, USA) from 2000 to 500 cm^{-1}.

Electrochemical measurements

The electrochemical measurements were performed in a three-electrode cell. To evaluate the electrochemical performances of these electrode materials, the working electrodes were an effective area of 20×20 mm^2 air electrode, a 50×10 mm^2 zinc sheet was used as the counter electrode. The electrolyte was 1.5 M NH_4Cl and 0.5 M CH_3COOH. Electrochemical impedance spectroscopy (EIS), EIS was carried out in the frequency ranging from 0.01 to 100,000 Hz at an open circuit potential with AC voltage amplitude of 5 mV. The potentiodynamic polarization curve is used to determine the relationship between electrode potential and current density, from 0 V to − 0.8 V (relative to open circuit potential), 2 mV/s. Polarization curve and EIS were measured by CHI660E Electrochemical Workstation (CHI660E, Shanghai Chenhua Device Company, China). Galvanostatic discharge curves were performed on a LAND-CT2001A cycle life tester (Wuhan Jinnuo Instrument Co Ltd., Wuhan, China) between 1.4 and 0.3 V.

All measurements were carried out at room temperature.

Results and discussion

Structures and morphologies

Figure 3 shows the infrared spectrum of the doped hydrochloric acid and the eigenstate polyaniline. The infrared absorption peak of polyaniline is mainly concentrated between 2000 and 500 cm^{-1} [34]. The absorption peaks of 1582 cm^{-1} and

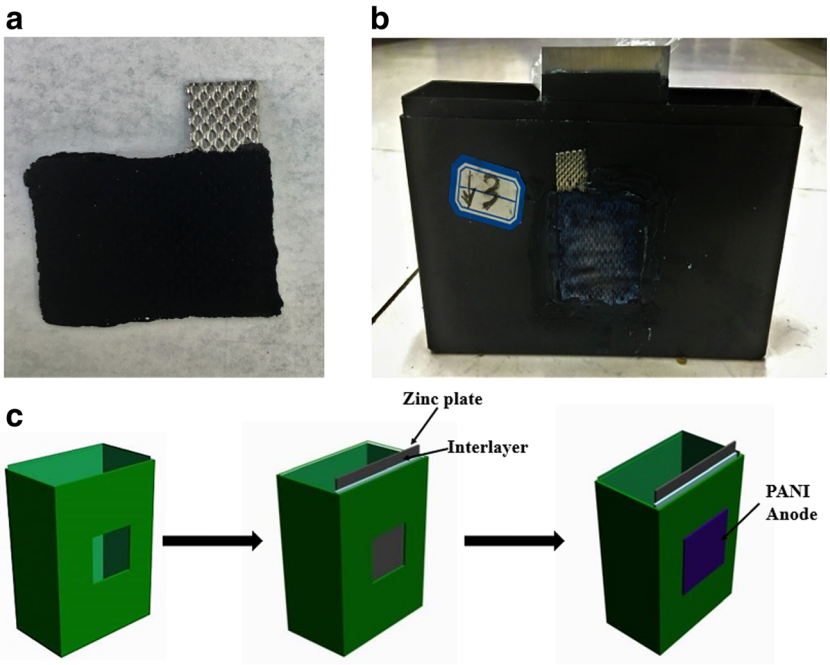

Fig. 2 Polyaniline anode (**a**) and battery device diagram (**b**, **c**)

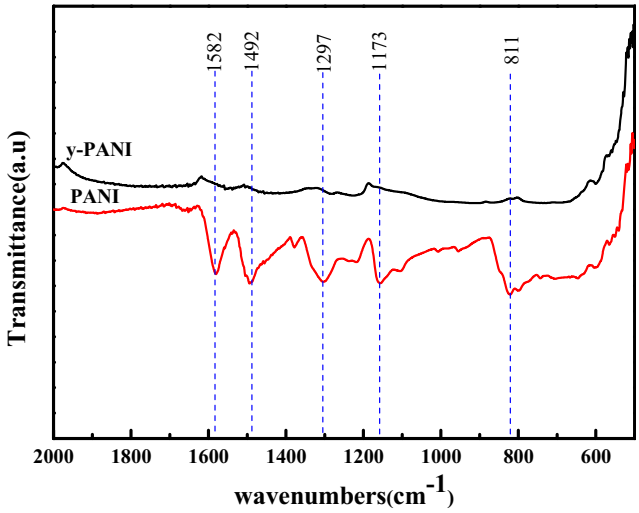

Fig. 3 FTIR spectra of PANI and y-PANI

1492 cm^{-1} correspond to the C=C stretching vibrations of the quinoid and benzene structures. 1297 cm^{-1} and 1173 cm^{-1} correspond to C–N and C=N stretching vibrations respectively, and the absorption peaks of these two functional groups belong to the characteristic absorption peak of polyaniline. The peak at 811 cm^{-1} was assigned to the stretching vibration of C–C. We can see from the infrared absorption peak curve of hydrochloric acid doped, after the proton acid doping, all the absorption peaks move to the low frequency direction, and the width of the peak becomes larger and the intensity of the peak becomes weaker especially the absorption peak of C=N. This is because the doping of protonic acid occurs on the N atom of the quinoid structure, resulting in a large change in atomic force and a decrease in the density of the electron cloud of the polyaniline molecular chain.

In order to study the relationship between the crystallinity of polyaniline and the polyaniline state, the polyaniline in different states was tested by XRD [35, 36]. From Fig. 4, we

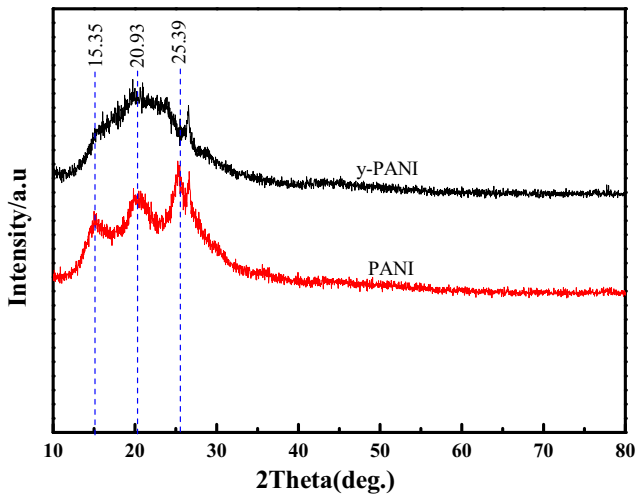

Fig. 4 XRD patterns of PANI and y-PANI

can see that the XRD diffraction peak of polyaniline prepared by the adsorption double oxidant method is mainly concentrated on $2\theta = 10° \sim 30°$. Among them, the eigenstate polyaniline has obvious diffraction peaks at $2\theta = 15.35°$, 20.93°, and 25.39° corresponding to the (011), (100), and (110) crystal planes of PANI, and the peak broadening of each diffraction peak can be attributed to the periodic distribution of polyaniline parallel and perpendicular to the molecular chain. The polyaniline doped with hydrochloric acid only has a distinct diffraction peak at $2\theta = 20.93°$, and the peak shape is sharper than the eigenstate, indicating that the polyaniline has higher crystallinity after doping. The sharper diffraction peak appearing at $2\theta = 28.34°$ corresponds to the diffraction peak of activated carbon.

As shown in Fig. 5, the morphologies of y-PANI, PANI, and the positive electrode were visually examined by FESEM. The nanostructure of PANI (Fig. 4a) was composed of nanofibers but in a denser clustered form compared with the y-PANI. And y-PANI is an agglomeration of nanofibers with large specific surface. It is provided that the specific capacity of polyaniline can be improved forming a stable polyaniline skeleton, which prepares conditions for rapid doping and dedoping of ions and charge transport. Therefore, we use polyaniline doped with hydrochloric acid (y-PANI) as the electrode material. Fig. 5c and Fig. 5d show that the fibrous PTFE connects the polyaniline particles together and has a certain pore structure, which facilitates the entry of air and improves the utilization of internal polyaniline.

Electrochemical properties

Most of the polyaniline synthesized by chemical oxidation and electrochemical synthesis are semi-oxidized states with $y = 0.5$ [37]. In order to verify the oxidation of the reduced polyaniline by air, we applied constant voltage for 10 mins to reduce the polyaniline membrane synthesized by electrochemical method to −0.8 V (vs SEE) in 1.5 M ammonium chloride and 0.5 M acetic acid solution. Then, the applied negative pressure was removed and the bubble was continuously bubbled and detect the potential change of the polyaniline film. As shown in Fig. 6, we can see that with the voltage removed, the potential of the polyaniline film rises rapidly, and when it reached a certain potential, it was going to slow down, and the potential of the bubbled polyaniline film was higher than the potential without bubbling, indicating that the contact with oxygen was favorable for the oxidation of the reduced polyaniline film. More benzene structures in polyaniline turned to oxime structures. Therefore, contact with sufficient oxygen is beneficial to the oxidation of polyaniline.

In order to study the impedance of the electrode, the battery was tested for AC impedance and the equivalent circuit was analyzed as shown where Rs represents the bulk resistance of the battery, reflecting the resistance of the electrode material,

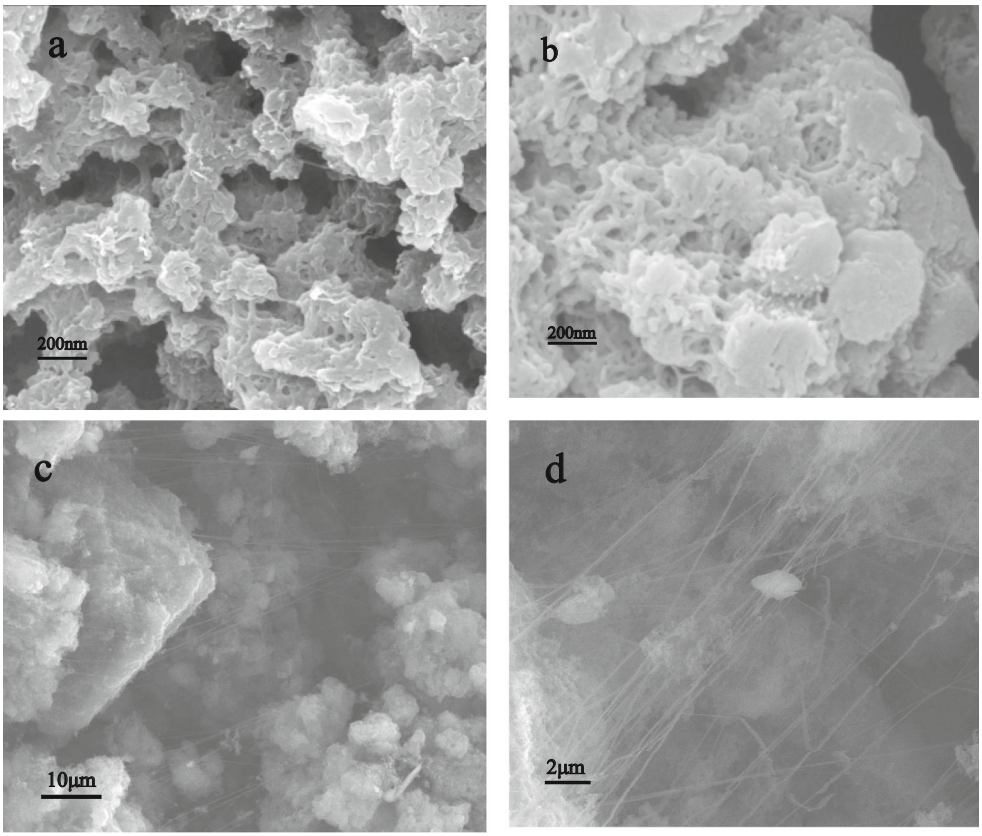

Fig. 5 FESEM images of y-PANI (**a**), PANI (**b**), and positive electrode (**c**, **d**)

diaphragm, and electrolyte; Rct and CPE represent the charge transfer resistance and the electric double layer capacitance, respectively, corresponding to the semi-circle of the intermediate frequency region. Figure 7 shows the Nyquist plots for each electrode. Pure polyaniline and polyaniline doped with a small amount of carbon Rct are relatively small, 21.19 Ω and 27.6 Ω, respectively, indicating that the electron transfer rate is faster when the material undergoes electrochemical reaction, which facilitates dedoping of ions and facilitates electrode reaction. The charge transfer resistance of the pure carbon electrode reaches 90.75 Ω, indicating that the carbon-catalyzed oxygen reduction reaction is difficult to occur under the ammonium chloride acidic electrolyte.

Figure 8 is a polarization curve measured by potentiodynamic scanning. The voltage drop of 0–30 mA/cm^2 is mostly caused by electrochemical polarization. We can see that the pure polyaniline and the PANI with small amount of carbon have higher electrochemical activity, the voltage drop is smaller, and the electrochemical reaction is easier to carry out. The

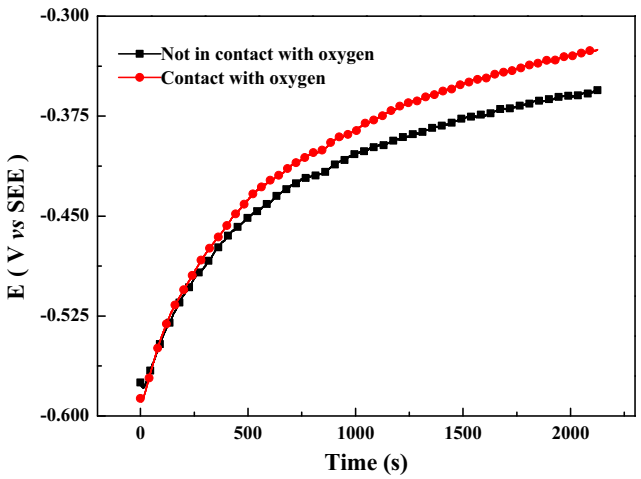

Fig. 6 Potential change of reduced PANI film

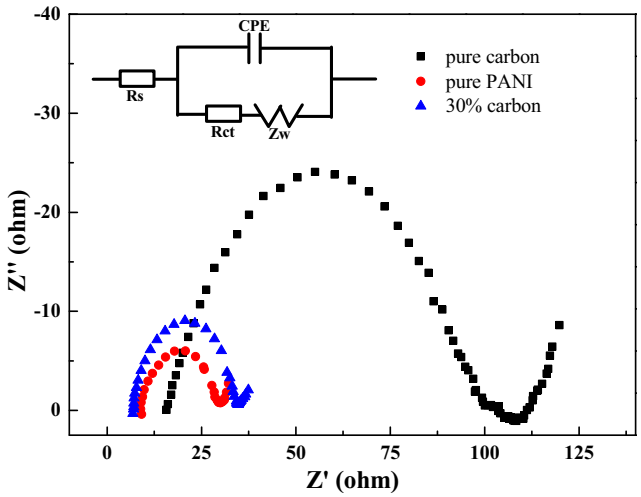

Fig. 7 Nyquist plots of pure carbon pure PANI and PANI with 30% carbon

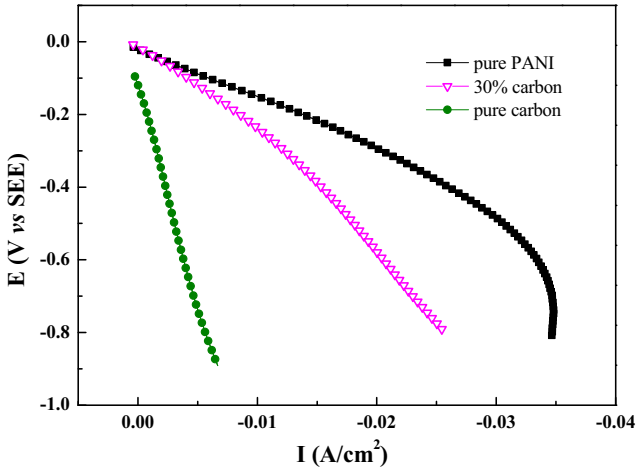

Fig. 8 Polarization curve of pure PANI, pure carbon, and 30% carbon electrode

voltage drop of pure carbon is large, and the electrode potential drops sharply.

In order to verify the discharge performance of the battery, galvanostatic discharge experiment of battery was carried out. When the cell discharged the voltage falls slowly until the PANI oxidized form is changed completely to its reduced form. Figure 10a shows the discharge curve of a traditional polyaniline electrode and a gas diffusion type polyaniline electrode at 10 mA. In contrast, the polyaniline is made into a hydrophobic gas permeable structure similar to an air electrode, which can greatly increase the discharge capacity of the battery and has a relatively stable discharge voltage (0.85 V). The excess discharge capacity is derived from the special oxygen reduction catalysis during discharge, from 150 to 1850 mAh/g. In the absence of contact with air, the polyaniline in the positive electrode is de-doped and the capacity is small. In the case where the positive electrode is in contact with air, we have found that the PH of the electrolyte rises significantly after a long period of discharge, which indicates that oxygen participates in the electrode reaction. The reaction principle of the battery is shown in Fig. 9. During the discharge process, zinc loses electrons, polyaniline electrons gradually become reduced polyaniline (r-PANI), and r-polyaniline contacts with oxygen in gas diffusion electrode, oxygen gets electrons in the positive electrode and the reduced polyaniline loses electrons and returns to PANI. Polyaniline acts as an intermediate (a special oxygen reduction catalyst) to promote the occurrence of oxygen reduction.

Furthermore, we did a set of repeated experiments to verify the large-capacity repeatability of the zinc–polyaniline battery assembled by this gas diffusion electrode, as shown in Fig. 10b. Although the discharge time and the voltage platform are slightly different from each other, the lowest discharge capacity is also above 1200 mAh/g. The slight difference may be affected by factors such as gas permeability caused by kneading, humidity, and distances between positive and negative, etc.

Figure 10c is a comparison of the discharge curves of a gas diffusion type pure polyaniline electrode and a polyaniline electrode which a small amount of activated carbon is added. We can see that the addition of a small amount of activated carbon can improve the discharge stability of the battery compared with pure polyaniline. In the initial 10 h of discharge, the pure polyaniline electrode has a higher discharge voltage, which is consistent to the polarization curve. In a short period of time, pure polyaniline has better conductivity and higher electrochemical activity, but as the discharge progresses, the voltage is attenuated, and with a small amount of carbon, the voltage stability is greatly improved, and it is maintained at 0.88 V and is used until the zinc flakes are used up. This is because a small amount of carbon can be used to composite polyaniline use activated carbon as a matrix, and polyaniline is synthesized on the surface of the substrate to increase the specific surface area of polyaniline, which has high diffusion rate and high utilization rate of active materials. Moreover, polyaniline has

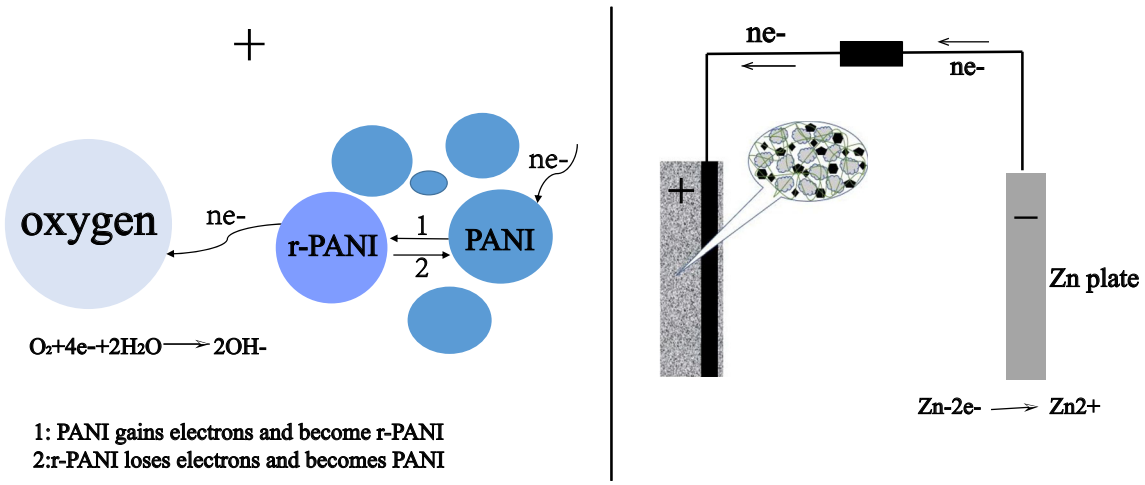

Fig. 9 Battery reaction schematic

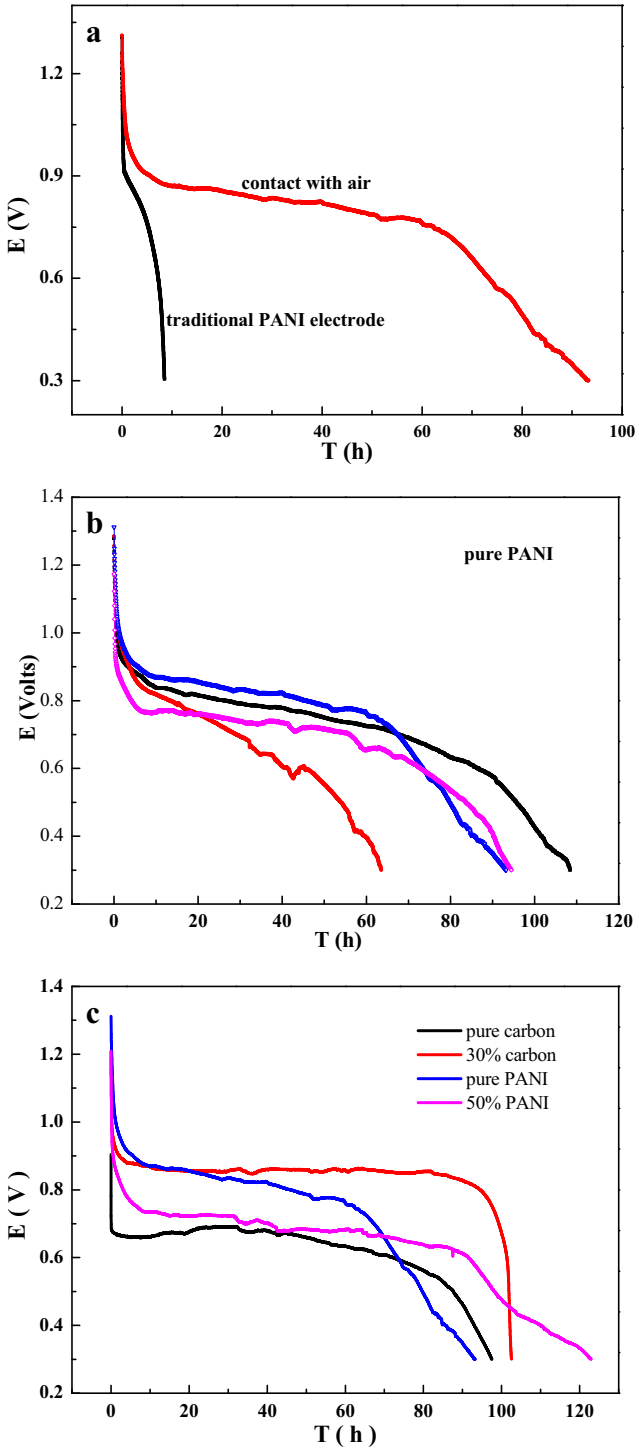

Fig. 10 Galvanostatic discharge curves at 10 mA

an O_2/N_2 separation coefficient of more than 50% and excellent oxygen permeability, and can catalyze oxygen reduction by auto-oxidation and reduction so that the electrode reactivity is greater than that of a pure carbon electrode. With the increase of exposed activated carbon, the lower the stable potential of the discharge curve is due to the poor ability of activated carbon to adsorb oxygen under acidic conditions, and it is difficult to catalyze oxygen reduction. Therefore, as the proportion of activated carbon increases, the voltage decreases.

Conclusion

In the acidic electrolyte, this paper successfully applied the gas diffusion electrode into the zinc–polyaniline battery, and the polyaniline which has reduced on the positive electrode in the discharge process can be slowly oxidized in the air contact to play the role in catalyzing oxygen reduction to achieve large capacity. Compared with the polyaniline battery, the discharge capacity is draply increased, and the capacity is increased by 10 times from 150 to 1850 mAh/g, and with the addition of a small amount of activated carbon, the battery life and discharge stability are more favorable.

References

1. Yang Z, Zhang J, Kintner-Meyer MCW, Lu X, Choi D, Lemmon JP, Liu J (2011) Electrochemical energy storage for green grid. Chem Rev 111(5):3577–3613
2. Zhai Y, Dou Y, Zhao D, Fulvio PF, Mayes RT, Dai S (2011) Carbon materials for chemical capacitive energy storage. Adv Mater 23(42):4828–4850
3. Goodenough JB (2013) Evolution of strategies for modern rechargeable batteries. Acc Chem Res 46(5):1053–1061
4. Cai S, Meng Z, Tang H, Wang Y, Tsiakaras P (2017) 3D Co-N-doped hollow carbon spheres as excellent bifunctional electrocatalysts for oxygen reduction reaction and oxygen evolution reaction. Appl Catal B 217:477–484
5. Ghanbari K, Mousavi MF, Shamsipur M, Karami H (2007) Synthesis of polyaniline/graphite composite as a cathode of Zn-polyaniline rechargeable battery. J Power Sources 170(2):513–519
6. Ćirić-Marjanović G (2013) Recent advances in polyaniline composites with metals, metalloids and nonmetals. Synth Met 170: 31–56
7. Yi L, Liu L, Guo G, Chen X, Zhang Y, Yu S, Wang X (2017) Expanded graphite@SnO2@ polyaniline composite with enhanced performance as anode materials for lithium ion batteries. Electrochim Acta 240:63–71
8. Zhang L et al (2017) Mn_3O_4/carbon nanotube nanocomposites recycled from waste alkaline Zn–MnO_2 batteries as high-performance energy materials. Rare Metals 36(5):442–448
9. Sun W, Wang F, Hou S, Yang C, Fan X, Ma Z, Gao T, Han F, Hu R, Zhu M, Wang C (2017) Zn/MnO_2 battery chemistry with H(+) and Zn(2+) coinsertion. J Am Chem Soc 139(29):9775–9778
10. Nam G, Park J, Choi M, Oh P, Park S, Kim MG, Park N, Cho J, Lee JS (2015) Carbon-coated core-shell Fe-Cu nanoparticles as highly active and durable electrocatalysts for a Zn–air battery. ACS Nano 9(6):6493–6501
11. Wei Z, Huang W, Zhang S, Tan J (2000) Carbon-based air electrodes carrying MnO_2 in zinc-air batteries. J Power Sources 91(2): 83–85
12. Dhavale VM, Kurungot S (2015) Cu-Pt nanocage with 3-D electrocatalytic surface as an efficient oxygen reduction electrocatalyst for a primary Zn-air battery. ACS Catal 5(3):1445–1452

13. Ma Z, Kan J (2013) Study of cylindrical Zn/PANI secondary batteries with the electrolyte containing alkylimidazolium ionic liquid. Synth Met 174:58–62
14. Huang J, Wang Z, Hou M, Dong X, Liu Y, Wang Y, Xia Y (2018) Polyaniline-intercalated manganese dioxide nanolayers as a high-performance cathode material for an aqueous zinc-ion battery. Nat Commun 9(1):2906
15. Fu Y, An Q, Ni R, Zhang Y, Li Y, Ke H (2018) Preparation of polyaniline-encapsulated carbon/copper composite nanofibers for detection of polyphenol pollutant. Colloids Surf A Physicochem Eng Asp 559:289–296
16. Oueiny C, Berlioz S, Perrin F (2014) Carbon nanotube-polyaniline composites. Prog Polym Sci 39(4):707–748
17. Bao C, He Q, Han J, Cheng J, Zhang R (2018) Functionalized graphene-polyaniline nanocomposite as electrode material for asymmetric supercapacitors. J Solid State Electrochim 22(9): 2917–2928
18. Zhang R et al (2018) Synthesis of PANI/rGO composite as a cathode material for rechargeable lithium-polymer cells. Ionics 24(11): 3367–3373
19. Wang Y, Wu X, Zhang W, Luo C, Li J, Wang Q, Wang Q (2018) Synthesis of polyaniline nanorods and Fe_3O_4 microspheres on graphene nanosheets and enhanced microwave absorption performances. Mater Chem Phys 209:23–30
20. Chen C, Gan Z, Xu C, Lu L, Liu Y, Gao Y (2017) Electrosynthesis of poly(aniline-co-azure B) for aqueous rechargeable zinc-conducting polymer batteries. Electrochim Acta 252:226–234
21. Chen C, Gan Z, Zhou K, Ma Z, Liu Y, Gao Y (2018) Catalytic polymerization of N-methylthionine at electrochemically reduced graphene oxide electrodes. Electrochim Acta 283:1649–1659
22. Yu J, Xie F, Wu Z, Huang T, Wu J, Yan D, Huang C, Li L (2018) Flexible metallic fabric supercapacitor based on graphene/polyaniline composites. Electrochim Acta 259: 968–974
23. Wu S, Zhao Y, Li D, Xia Y, Si S (2015) An asymmetric Zn//Ag doped polyaniline microparticle suspension flow battery with high discharge capacity. J Power Sources 275:305–311
24. Xia Y, Zhu D, Si S, Li D, Wu S (2015) Nickel foam-supported polyaniline cathode prepared with electrophoresis for improvement of rechargeable Zn battery performance. J Power Sources 283:125–131
25. Rahmanifar MS, Mousavi MF, Shamsipur M, Ghaemi M (2004) What is the limiting factor of the cycle-life of Zn-polyaniline rechargeable batteries? J Power Sources 132(1):296–301
26. Liu P, Han JJ, Jiang LF, Li ZY, Cheng JN (2017) Polyaniline/multi-walled carbon nanotubes composite with core-shell structures as a cathode material for rechargeable lithium-polymer cells. Appl Surf Sci 400:446–452
27. Male U, Modigunta JKR, Huh DS (2017) Design and synthesis of polyaniline-grafted reduced graphene oxide via azobenzene pendants for high-performance supercapacitors. Polymer 110:242–249
28. Pan J, Xu YY, Yang H, Dong Z, Liu H, Xia BY (2018) Advanced architectures and relatives of air electrodes in Zn-air batteries. Adv Sci (Weinh) 5(4):1700691
29. Zhu WH, Poole BA, Cahela DR, Tatarchuk BJ (2003) New structures of thin air cathodes for zinc-air batteries. J Appl Electrochem 33(1):29–36
30. Yang C (2004) Preparation and characterization of electrochemical properties of air cathode electrode. Int J Hydrog Energy 29(2):135–143
31. Sun T, Xu L, Li S, Chai W, Huang Y, Yan Y, Chen J (2016) Cobalt-nitrogen-doped ordered macro-/mesoporous carbon for highly efficient oxygen reduction reaction. Appl Catal B 193(1–8):1–8
32. Li BB, Liang YQ, Yang XJ, Cui ZD, Qiao SZ, Zhu SL, Li ZY, Yin K (2015) MoO_2-CoO coupled with a macroporous carbon hybrid electrocatalyst for highly efficient oxygen evolution. Nanoscale 7(40):16704–16714
33. Wang J, Wu Z, Han L, Lin R, Xiao W, Xuan C, Xin HL, Wang D (2016) Nitrogen and sulfur co-doping of partially exfoliated MWCNTs as 3-D structured electrocatalysts for the oxygen reduction reaction. J Mater Chem 4(15):5678–5684
34. Ghanbari K, Mousavi MF, Shamsipur M, Rahmanifar MS, Heli H (2006) Change in morphology of polyaniline/graphite composite: a fractal dimension approach. Synth Met 156(14):911–916
35. Jozefowicz ME, Laversanne R, Javadi HHS, Epstein AJ, Pouget JP, Tang X, MacDiarmid AG (1989) Multiple lattice phases and polaron-lattice-spinless-defect competition in polyaniline. Phys Rev B Condens Matter 39(17):12958–12961
36. Pouget JP, Jozefowicz ME, Epstein AJ, Tang X, MacDiarmid AG (1991) X-ray structure of polyaniline. Macromolecules 24(3):779–789
37. Ghani S, Sharif R, Shahzadi S, Zafar N, Anwar AW, Ashraf A, Zaidi AA, Kamboh AH, Bashir S (2015) Simple and inexpensive electrodeposited silver/polyaniline composite counter electrodes for dye-sensitized solar cells. J Mater Sci 50(3):1469–1477